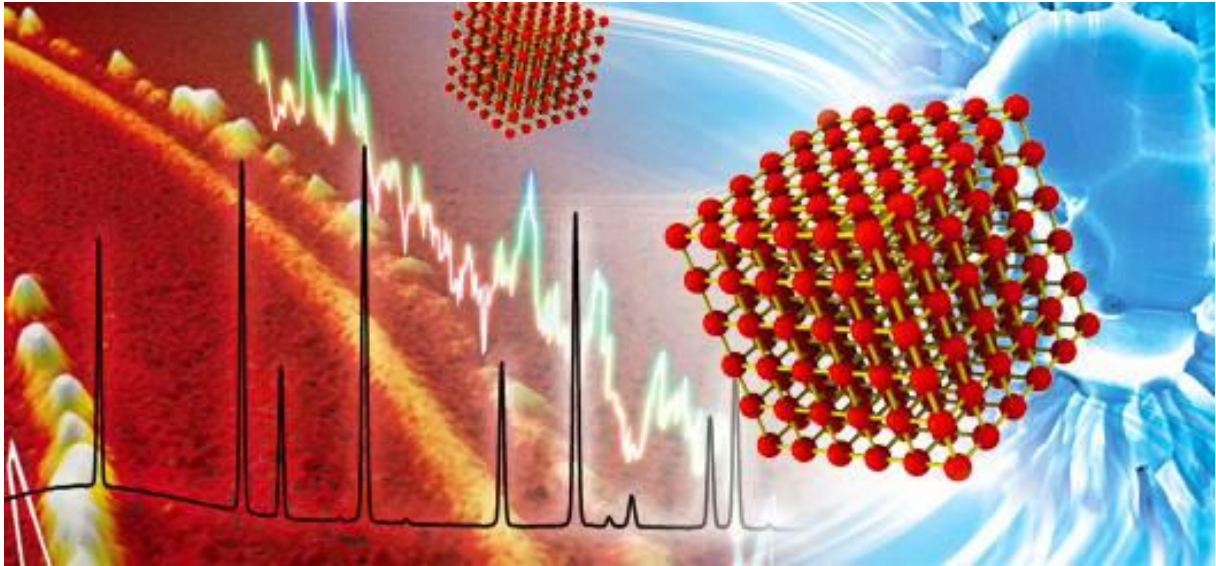


X-ray Diffraction of Semiconductor Heterostructures



Practical Course in the frame of the
Ferienpraktikum

Supervisor: Gregor Mussler, Jülich Spring 2020

1. Introduction

X-ray diffraction (XRD) is a powerful and versatile technique to characterize crystals. XRD employs elastic scattering of monochromatic x-ray light at atoms of the crystal, which will subsequently constructively interfere. From the geometrical arrangement of the sample and the detector, information of the crystal are obtained. The information include:

- Crystal structure
- Lattice constants
- Alloy concentrations
- Strain status
- Film thicknesses
- Interdiffusion processes

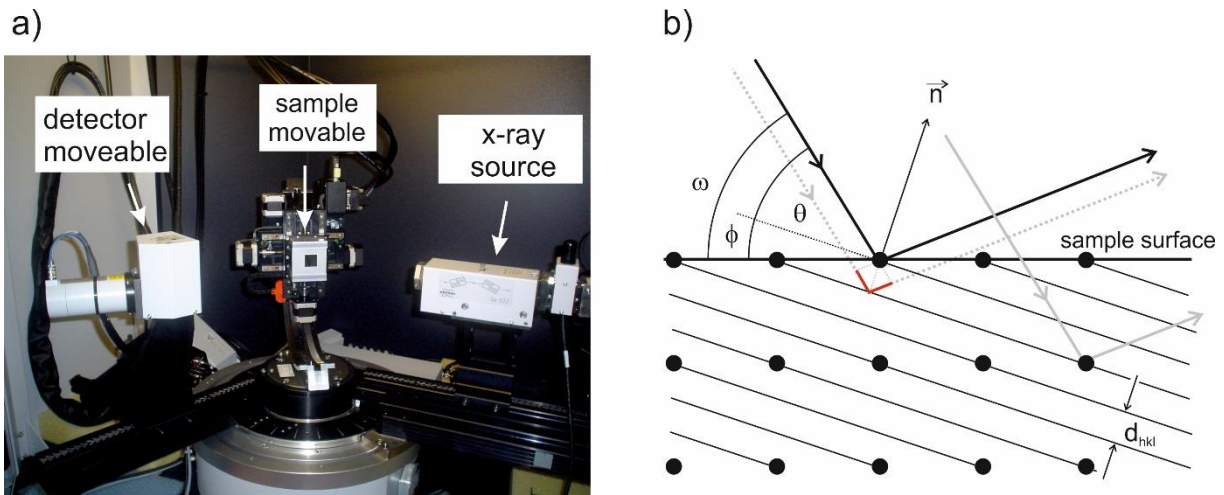


Fig 1: Photograph of the XRD system employed for this lab course (a). Geometrical arrangement of the XRD technique, including the crystal structure, the incoming and outgoing x-ray beams, and the investigated net planes (b).

Figure 1 a) shows the XRD system used in the lab course. It consist of a x-ray source, a sample holder, and a detector. In the x-ray source is built of a copper block, on which high energy electrons impinge upon ($U = 40$ kV). When the electrons enter the copper block, they are decelerated emitting a continuous spectrum of electromagnetic radiation, so called Bremsstrahlung. Besides, emission of discrete lines also takes place by means of excitations within the copper atoms, i.e. the $\text{Cu } K\alpha_1$ radiation with a distinct wavelength $\lambda = 1.54062 \text{ \AA}$. This monochromatic radiation is used for the XRD experiments. In order to filter out the $\text{Cu } K\alpha_1$ radiation, the x-ray source is equipped with a 4-crystal Ge monochromator, i.e. 4 Ge single crystals that are cut and aligned to employ the (022) reflection, which corresponds to the $\text{Cu } K\alpha_1$ wavelength. For the XRD scans, the sample on the sample stage and the detector are rotated with an angular resolution of 0.001° . The latter is equipped with mechanical slits as well as an additional Ge monochromator in order to obtain a very high detector resolution.

XRD is based on constructive interference of x-ray light on net planes. A theoretical description of constructive interference on net planes (h,k,l) is illustrated in figure 1 b). Here two coherent x-ray beams with wavelength λ (colored black and gray) impinge on net planes with distance d_{hkl} under the angle θ are shown, whereas the gray x-ray beam travels a longer distance $L = 2d_{hkl} \sin(\theta)$, as illustrated by the red line in Fig. 1 b). Constructive interference is obtained if the change in distance between the two x-ray beams L is multiple of the wavelength λ :

$$m\lambda = 2d_{hkl} \sin(\theta), \quad m = 1,2,3, \dots \quad [1]$$

Equation 1 is the Bragg equation, and is employed to find the geometrical arrangement (angle θ) to measure x-ray signals of these net planes.

Apart from dealing with net planes in real space, another very elegant way to carry out XRD is to work in the reciprocal space. Assuming a crystal represented by the Bravais lattice vectors $(\vec{a}_1, \vec{a}_2, \vec{a}_3)$, the corresponding reciprocal vectors $(\vec{b}_1, \vec{b}_2, \vec{b}_3)$ are defined as follows:

$$\vec{b}_1 = 2\pi \frac{\vec{a}_2 \times \vec{a}_3}{\vec{a}_1 \cdot (\vec{a}_2 \times \vec{a}_3)}, \quad \vec{b}_2 = 2\pi \frac{\vec{a}_3 \times \vec{a}_1}{\vec{a}_2 \cdot (\vec{a}_3 \times \vec{a}_1)}, \quad \vec{b}_3 = 2\pi \frac{\vec{a}_1 \times \vec{a}_2}{\vec{a}_3 \cdot (\vec{a}_1 \times \vec{a}_2)} \quad [2]$$

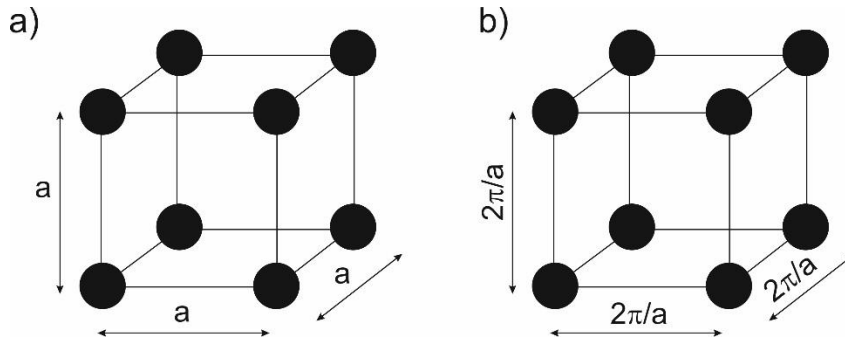


Fig 2: Cubic crystal structure in real space (a) and in reciprocal space (b).

Figure 2 depicts the Bravais lattice vectors of a cubic crystal (a) with lattice constant a (e.g. Si, Ge, GaAs, InP, ...) and their reciprocal lattice vectors (b). It turns out (unlike many other crystals) that the reciprocal lattice of a cubic crystal is again a cubic crystal with a reciprocal lattice constant $2\pi/a$. The reciprocal lattice vector \vec{K}_{hkl} is now very useful to define the XRD scan around the (h,k,l) reflection, which is equivalent to a XRD scan at the (h,k,l) net plane:

$$\vec{K}_{hkl} = h\vec{b}_1 + k\vec{b}_2 + l\vec{b}_3 \quad [3]$$

A very beneficial property of \vec{K}_{hkl} is the fact that it stands perpendicular to the (h,k,l) netplanes and its magnitude is inversely proportional to the net spacing d_{hkl} :

$$d_{hkl} = \frac{2\pi}{|\vec{K}|} \quad [4]$$

Employing equations 3 and 4, it is now possible to determine the Bragg angle θ for a reflection (h,k,l) for cubic crystals. In a similar fashion, it is also possible to determine the tilt angle ϕ between the net planes and the sample surface (cf. fig 1 b). Assuming a (m,n,o)-oriented surface, the reciprocal vector \vec{K}_{mno} that stands perpendicular to the sample surface:

$$\vec{K}_{mno} = m\vec{b}_1 + n\vec{b}_2 + o\vec{b}_3 \quad [5]$$

Recalling that \vec{K}_{hkl} stands perpendicular to the net planes (h,k,l), the angle between net planes and the sample surface is simply the angle between the two vector \vec{K}_{hkl} and \vec{K}_{mno} :

$$\varphi = \cos^{-1} \left(\frac{\vec{K}_{hkl} \cdot \vec{K}_{mno}}{|\vec{K}_{hkl}| \cdot |\vec{K}_{mno}|} \right) \quad [6]$$

In order to carry out XRD scans in the reciprocal space, two different scan types have to be distinguished: ω scans and $\omega/2\theta$ scans. Fig 3 depicts these two different scans. It is seen that in case of ω scans (i.e. only the sample is moved, the detector remains fixed, c.f. fig 1 a), the scan direction is parallel to the net planes. In contrast, the scan direction of $\omega/2\theta$ scans is perpendicular to the net planes. Hence, by carrying out $\omega/2\theta$ scans in dependence of ω results in a 2-dimensional map of the reciprocal space.

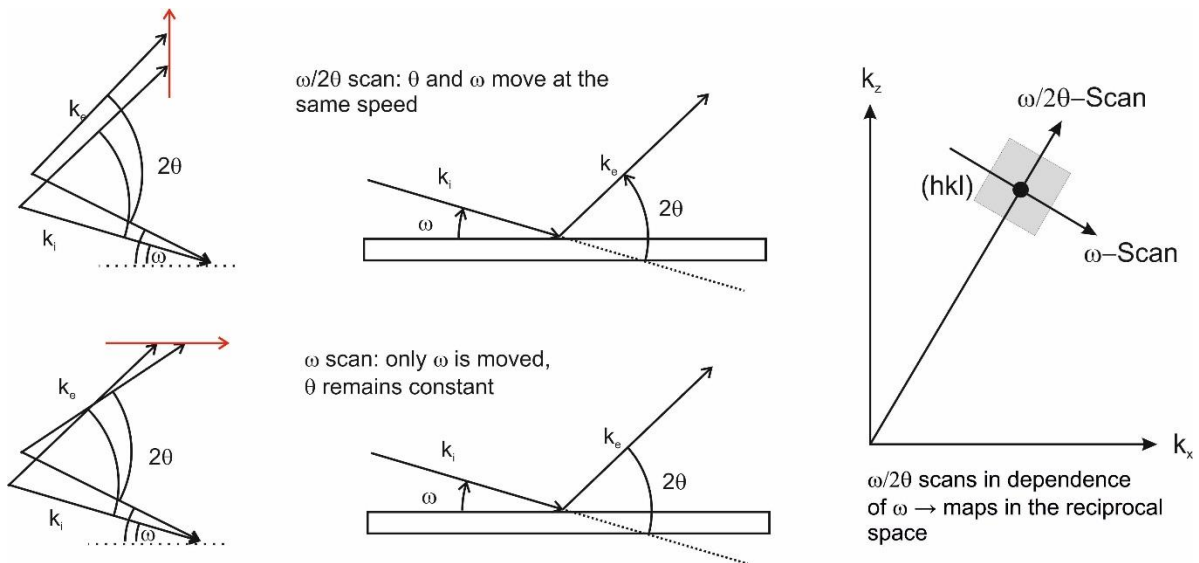


Fig 3: Schematics of the geometrical arrangement of ω scans, $\omega/2\theta$ scans, and reciprocal space maps.

Plain geometrical considerations are applied to convert the angles ω and θ into reciprocal lattice vectors k_x and k_z . Fig. 4 shows the geometrical arrangement in real space (a) and reciprocal space (b). Here the difference k-vector K between incident beam k and diffracted beam k' is decomposed into its k_x and k_z component:

$$|\vec{K}| = 2|\vec{k}| \sin \theta = \frac{4\pi}{\lambda} \sin \theta \quad [7]$$

$$K_x = K \sin(\theta - \omega) = \frac{4\pi}{\lambda} \sin \theta \sin(\theta - \omega) \quad [8]$$

$$K_y = K \cos(\theta - \omega) = \frac{4\pi}{\lambda} \sin \theta \cos(\theta - \omega) \quad [9]$$

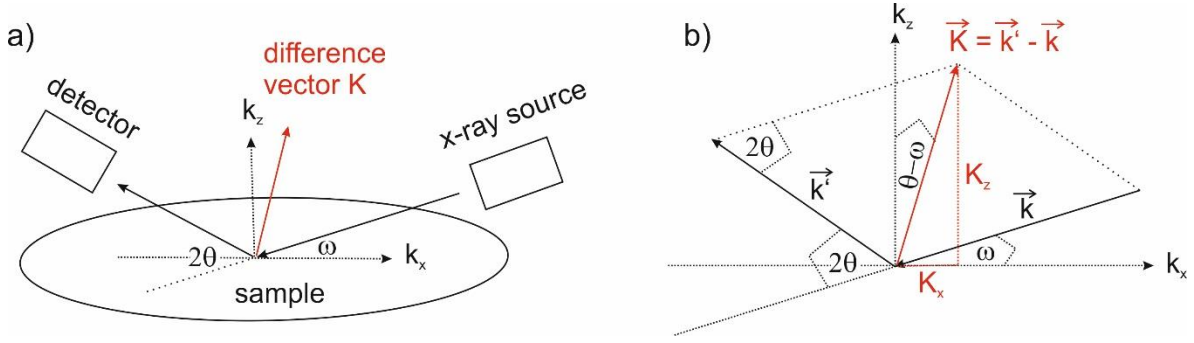


Fig 4: Geometry of incoming and outgoing x-ray beams, including the experimental angles ω and θ .

Reciprocal space maps are important to determine the strain status of heteroepitaxial layers. Fig. 5 shows two crystal structures of epilayers grown on a substrate with different lattice constants as well as their reciprocal space maps. Fig. 5 a illustrates the fully strained case, i.e. the in-plane lattice constant of the epilayer a_{\parallel} matches the lattice constant of the underlying substrate a_s . As a consequence, the out-of-plane lattice constant a_{\perp} is elongated with respect to the unstrained case, as it will be discussed in the next section. The fact that $a_{\parallel} = a_s$ is seen in the reciprocal space map (Fig 5 c), as the peaks of substrate and epilayer have the same k_x value. Figure 5 b illustrates the fully relaxed case. Relaxation processes occur for epilayers with thicknesses exceeding a certain critical thickness as a consequence of energy minimization. In this case, dislocations at the interface between substrate and epilayer are formed, and the epilayer's lattice constants will change towards its bulk values $a_{\parallel} = a_{\perp} = a_0$. As a result, the epilayer's peak is moved in the reciprocal space, i.e. it is no longer located at the k_x position of the substrate but it is shifted towards lower k_x values (corresponding to a larger in-plane lattice constant). Correspondingly, the out-of-plane lattice constant a_{\perp} is not elongated anymore – as in the strained case, and the epilayer peak is now located at larger k_z values.

In order to revert the (k_x, k_z) reciprocal lattice vector, one has to recall that the reciprocal lattice vector is inversely proportional to the lattice constant (equation 7). Rewriting equation 7 yields:

$$K_{hkl}^2 = \frac{4\pi^2}{d_{hkl}^2} = 4\pi^2 \left(\frac{h^2 + k^2}{a_x^2} + \frac{l^2}{a_z^2} \right) = K_x^2 + K_z^2 \quad [10]$$

In the third term in equation 10, the equation of d_{hkl} of biaxially strained cubic crystals was employed. In the last term in equation 10, Pythagorean theorem is used. Comparing the last two terms, and taking into account that K_x and K_z only depend on $a_x (= a_{\parallel})$ and $a_z (= a_{\perp})$ respectively, the following equations are derived:

$$k_x^2 = 4\pi^2 \left(\frac{h^2 + k^2}{a_x^2} \right) \rightarrow a_x = \frac{2\pi}{k_x} \sqrt{h^2 + k^2} \quad [11]$$

$$k_z^2 = 4\pi^2 \left(\frac{l^2}{a_z^2} \right) \rightarrow a_z = \frac{2\pi}{k_z} l \quad [12]$$

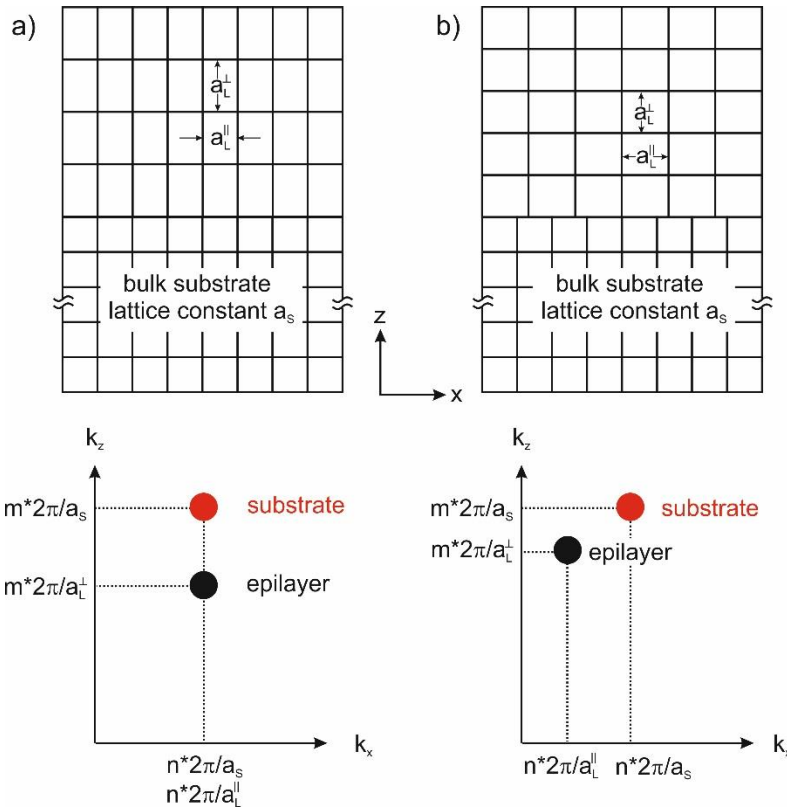


Fig 5: Crystal structures in real space and their reciprocal space maps of a fully strained (a) and a fully relaxed epilayer (b) grown on a substrate with a smaller lattice constant.

Apart from the band gap, the lattice constant of semiconductors is the most important properties. Growing semiconductor film on top of substrate with a different lattice constant – the so called heteroepitaxy – may cause strain in the epilayer. Figure 6 shows the band gap of several semiconductors in dependence of the lattice constant. Such maps are important for device engineers, as it illustrates what configurations of epilayer/substrates are allowed to be harnessed in devices.

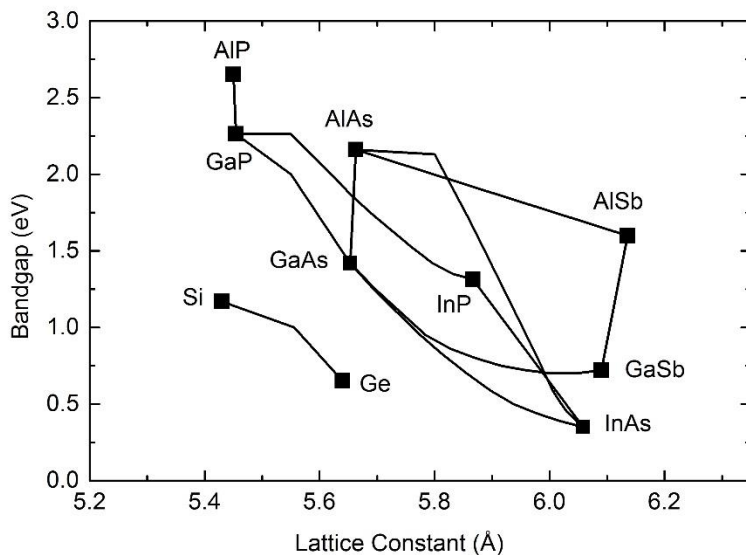


Fig 6: The “semiconductor works map”, i.e. the lattice constant vs. band gap of several elemental and compound semiconductors.

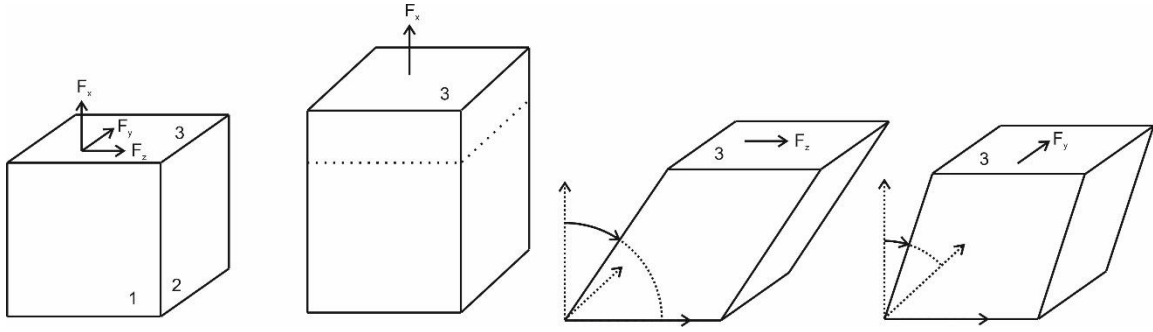


Fig 7: Sketch of a cubic crystal that is distorted by a force acting on plane 3 in x- y- and z-direction.

In order to determine the distortion strain may cause, the theory of elasticity is applied. Similar to the case of a one-dimensional spring, the basic idea here is that the repulsive force is linear to the elongation (Hooke's law: $F = -C\Delta x$, where C is the spring constant). However, in case of a three-dimensional crystal, the quantity C now becomes a tensor. Let us consider a cubic crystal as depicted in Fig 7. The crystal has a total of three planes (denoted 1,2, and 3), and forces in three different directions (denoted F_x , F_y , and F_z) may act upon each plane. Hence, we have to distinguish between 9 different cases. Let us define the strain tensor ε_{kl} (force per unit area) and the stress tensor σ_{ij} (relative displacement of atoms from their equilibrium position). Now Hooke's law reads:

$$\sigma_{ij} = \sum_{kl} C_{ijkl} \varepsilon_{kl} \quad [13]$$

With C_{ijkl} is the elasticity tensor. Since ε_{kl} and σ_{ij} have each 9 components, C_{ijkl} has a total of 81 components. Fortunately, symmetry considerations strongly reduce the components of C_{ijkl} , and for cubic crystals with (0,0,1) orientation, only C_{11} and C_{12} are completely independent. Furthermore, by calculating the elastic energy of the strained crystal with unstrained lattice constant a_0 , the following relationship between $\varepsilon_{xx} == \varepsilon_{||}$ and $\varepsilon_{zz} == \varepsilon_{\perp}$ is derived:

$$\varepsilon_{||} = \frac{a_{||} - a_0}{a_0}, \varepsilon_{\perp} = \frac{a_{\perp} - a_0}{a_0}, \varepsilon_{\perp} = -2 \frac{C_{12}}{C_{11}} \varepsilon_{||} \quad [14]$$

The minus sign in equation 14 dictates that the change of the out-of-plane lattice constant is always opposite with respect to the change of the in-plane lattice constant, i.e. a compressive in-plane strain ($a_{||}$ becomes smaller) leads to a larger a_{\perp} and vice versa. As a rule of thumb, the volume of the strained crystal is nearly constant, irrespective of the strain. Solving equation 14 for a_0 yields:

$$a_0 = \frac{a_{\perp} + \nu a_{||}}{1 + \nu}, \nu = 2 \frac{C_{12}}{C_{11}} \quad [15]$$

Silicon (Si) is regarded as on the most important material in our information society, and some historian even call the 20th century the Si age, as many devices of every days life are based on Si. Examples that stress the importance of Si include integrated circuits in computers, CCD chips found in digital cameras, and solar panels that become more and more important for the energy generation. Apart from bulk Si,

many application show better device performance in case if strained Si. For example, strain in the Si crystal causes a warping of the band structure, which causes a lower effective electron mass and subsequently a higher mobility. In fact, some high-end Si transistors are now based on strained Si. A possible avenue to create strain in Si is to grow Si layer on Si_{0.5}Ge_{0.5} pseudosubstrates. Some important parameters of Si and Ge are listed in table 1.

Material	Band gap	Lattice constant	C ₁₁ (dyn/cm ²)	C ₁₂ (dyn/cm ²)
Silicon	1.2 eV (indirect)	5.431 Å	16.6x10 ¹¹	6.4x10 ¹¹
Germanium	0.67 eV (indirect)	5.659 Å	12.6x10 ¹¹	4.4x10 ¹¹

Table 1: Basic parameters of the semiconductor Si and Ge.

Table 1 shows that Si and Ge have different lattice constants. Regarding the lattice constant of the Si_{1-x}Ge_x alloy, a linear interpolation, the so-called Vegard's law, may be employed:

$$a_{SiGe} = (a_{Ge} - a_{Si}) \cdot x_{Ge} + a_{Si} \quad [16]$$

More sophisticated model employ a bowing parameter to determine the lattice constant of Si_{1-x}Ge_x, the so-called Dismukes law: Si_{1-x}Ge_x

$$a_{SiGe} = a_{Si} + 0.20 \cdot x_{Ge} + 0.027 \cdot x_{Ge}^2 \quad [17]$$

Figure 8 shows a cross-section of a Si_{0.5}Ge_{0.5} pseudosubstrate, measured by means of transmission electron microscopy. It consists of a Si substrate, on which a several μm thick SiGe buffer layer is grown. As there is a large lattice mismatch between Si and Ge ($\Delta a/a = 4.2\%$, c.f. figure 6), the SiGe buffer layer eventually relaxes for thicker layers and higher Ge content. The buffer layer is grown at optimized growth recipes (i.e. the Ge content was gradually increased to the final Ge content of 50%) in order to keep the dislocation that are formed during the relaxation process, close to the interface between the Si substrate and the SiGe buffer layer. On top of the buffer layer, a Si_{0.5}Ge_{0.5} cap layer is grown. Figure 8 b shows a reciprocal space map (RSM) of such SiGe pseudosubstrate. Three features are seen in the map: the Si substrate peak, the graded SiGe buffer layer, and the Si_{0.5}Ge_{0.5} cap layer. From the (k_x, k_z) coordinates of the SiGe cap layer peak, the in-plane and out-of-plane lattice constants are derived, which are subsequently used to determine the Ge content x_{Ge} and the strain status $\epsilon_{||}$ and ϵ_{\perp} .

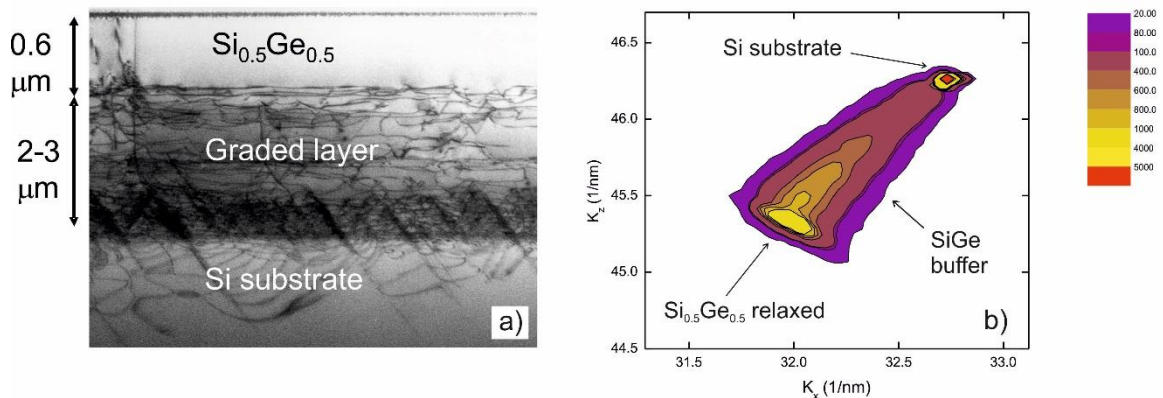


Fig 8: Cross-sectional transmission electron microscopy image of a SiGe pseudosubstrate (a). Reciprocal space map of this particular SiGe pseudosubstrates (b).

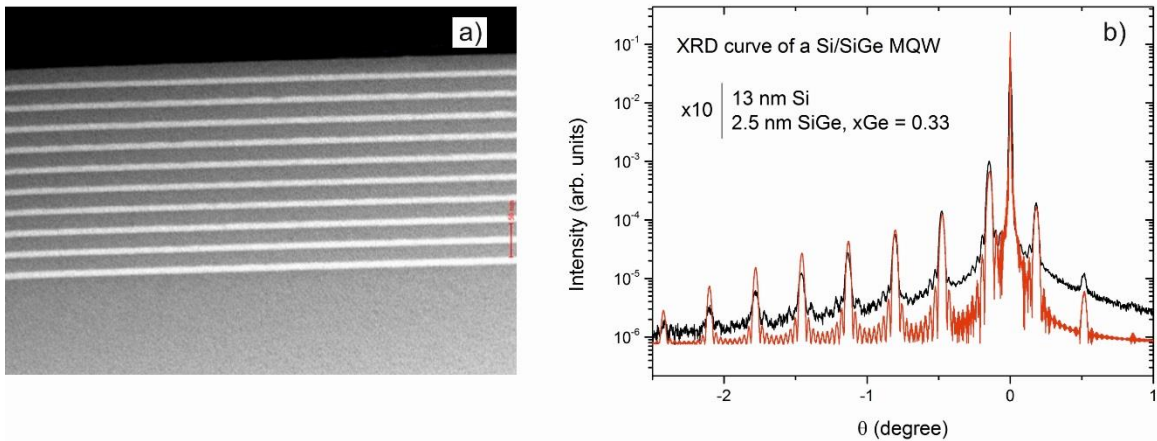


Fig . 9: a) Transmission electron microscopy image of a 10-period SiGe/Si multiple quantum well structure. The SiGe quantum wells (Si barriers) are the bright (dark) stripes. b) XRD curve of the superlattice shown in the TEM image.

Another type of semiconductor heterostructures are multiple quantum wells or superlattices. They consist of alternating sequences of layers with different materials, usually called barrier (material with a large band gap) and quantum well (material with a small band gap). Such superlattices are extremely important for devices, as carriers are confined in the barriers which leads to a higher mobility of electrons and hole – beneficial for example in transistor applications , or to a more pronounced radiative recombination of electrons and holes for example in laser applications. Such superlattices are grown in sophisticated deposition systems, such as molecular beam epitaxy or chemical vapor deposition. Figure 9 depicts a transmission electron microscopy image of a 10-period SiGe/Si multiple quantum well structure.

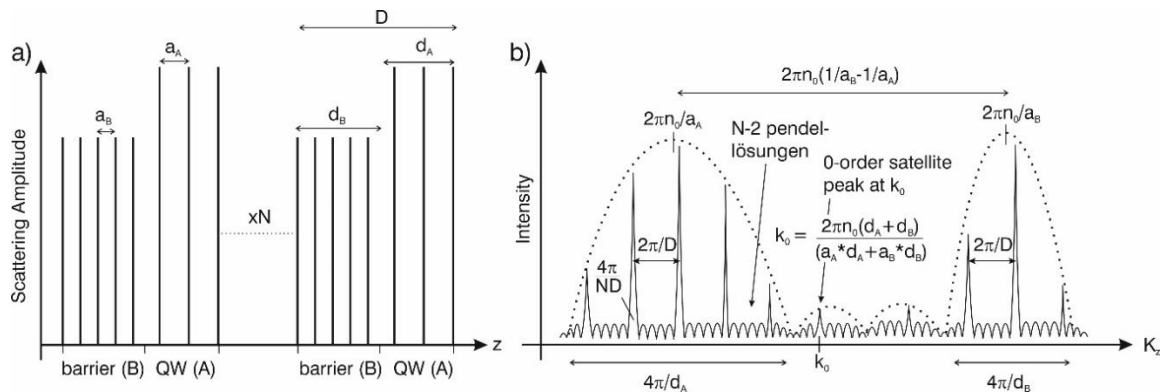


Fig 10: The scattering factors of a superlattice in real space (a) and its Fourier transform, i.e. its XRD curve (b).

XRD $2\theta/\theta$ scans are a powerful technique to analyze these superlattices. Let us consider the form factor distribution in real space, as illustrated in Fig. 10 a. By carrying out an XRD scan, the measured intensity profile is simply the Fourier transform of the form factor distribution. The XRD curve, i.e. the Fourier transform (in reciprocal space) of the form factors in real space, is shown in Fig 10 b. The XRD curve consists of several features, such as satellite peaks, envelopes, and pendellösung fringes. By employing analytical consideration, the following sample parameters are obtained (c.f. Fig 10 b):

- Lattice constant of QW and barrier \leftrightarrow K position of central Bragg peak of QW or barrier
- QW or barrier thickness \leftrightarrow Width of QW or barrier envelope
- Thickness of barrier/QW \leftrightarrow Distance between adjacent satellite peaks
- Number of QW/barrier stacks \leftrightarrow Number of pendellösung fringes
- Total thickness of superlattice \leftrightarrow Width of individual satellite peak
- Average lattice constant of QW and barrier \leftrightarrow Position of zero-order satellite peak

In principle, it is possible to determine all the sample parameter analytically from the equation depicted in Fig 10 b. However, nowadays computer programs, based on the dynamical theory, are used to simulate the XRD curves and to obtain the structural parameters described above.

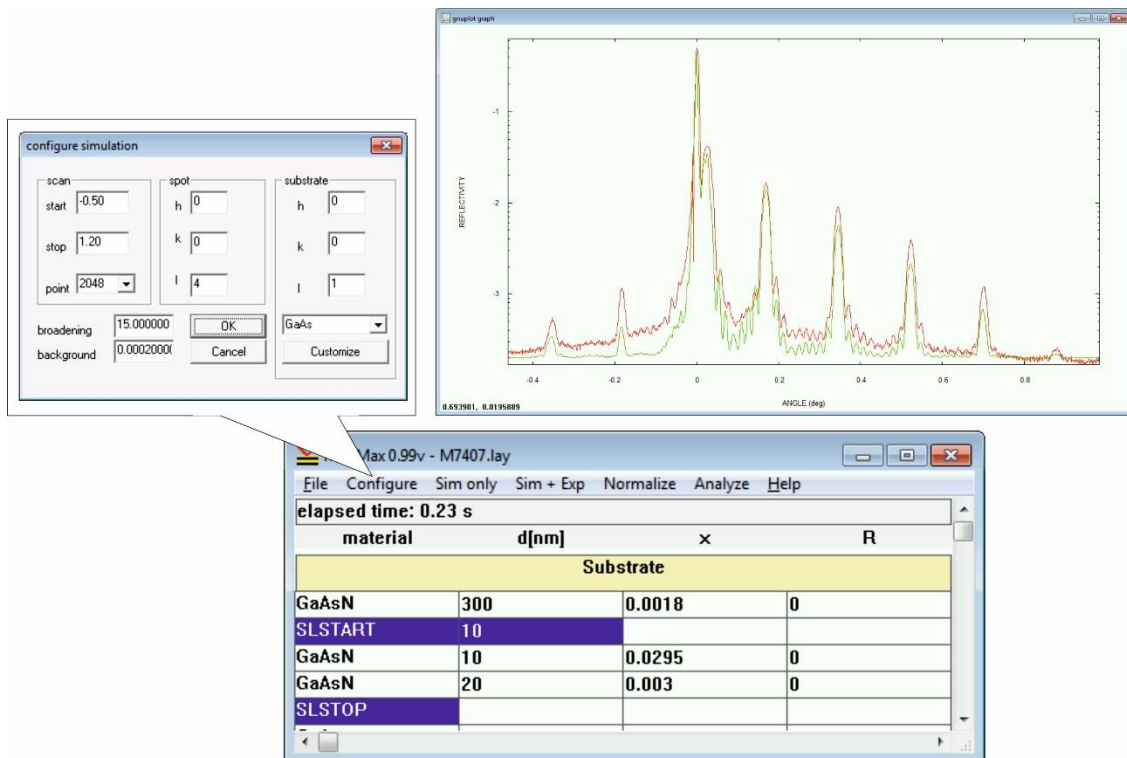


Fig 11: Screenshot of the software “MadMax” that is used to simulate XRD curves.

Fig. 11 shows a screenshot of the program “MadMax” that is used to simulate the XRD curve. In the bottom window, the structure – in this case a GaAs/GaAsN multiple quantum well - is inserted. In the top window on the left hand side, the investigated reflection, the substrate, the substrate orientation, and the scan range are inserted. By punching the “Sim + Exp” button, the window on the right hand side pops up, showing the experimental curve (red) and the simulation (green).

So far, we have only discussed diffraction of x-ray on net planes. However, x-rays may also be suitable to carry out diffraction upon the surface and interface of a thin film grown on substrate. This technique is called x-ray reflectivity (XRR). In XRR, incoming and outgoing x-ray beam are aligned at very small angles ($\theta = 0 - 5^\circ$). Figure 12 depicts a XRR curve of a 31 nm thick Bi_2Te_3 film grown on a Si substrate. The inset of Fig. 12 illustrates the geometrical arrangement of a XRR experiment. In principle, one can now use the Bragg equation (equation 1) to determine the film thickness. However, unlike for XRD experiments that are carried out at large angles, the dispersion of x-ray light with respect to the sample material has to be taken into account, i.e. the angle of incidence θ is altered to θ' within the sample

(see inset of Fig. 12). It turns out that for electromagnetic radiation with extremely high frequencies (such as x-rays), the refractive index is only a tiny fraction smaller than 1 in the order of $\delta = 10^{-5}$.

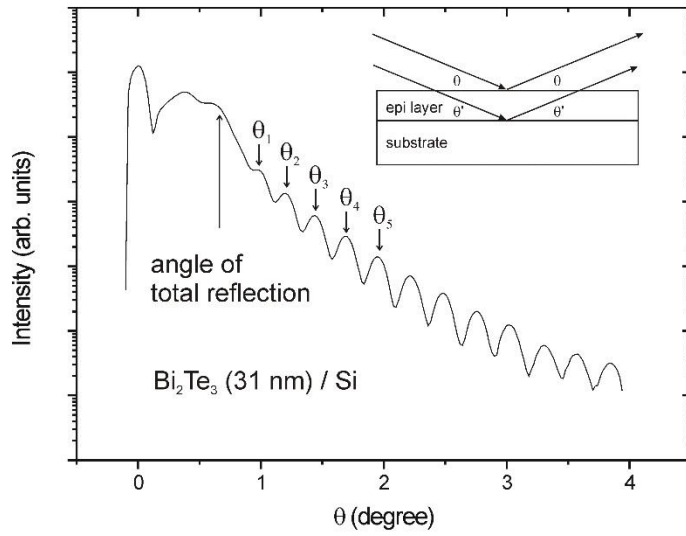


Fig 12: an XRR curve of a Bi_2Te_3 film grown on s Si substrate. The inset illustrates the geometrical arrangement of the XRR setup.

Hence the refractive index n of x-ray light reads:

$$n = 1 - \delta \quad [18]$$

Taking Snell's law into account, one can easily derive an equation to determine the internal angle θ' :

$$\theta' = \cos^{-1} \left(\frac{\cos \theta}{1 - \delta} \right) \quad [19]$$

Hence, due to dispersion, the Bragg equation is slightly modified by a correction term:

$$m\lambda = 2d \sin(\theta_m) \sqrt{1 - \frac{2\delta}{\sin^2(\theta_m)}} \quad [20]$$

Solving equation 20 for $\sin^2(\theta_m)$ reads:

$$\sin^2(\theta_m) = \frac{\lambda^2}{4d^2} m^2 + 2\delta \quad [21]$$

Hence, plotting $\sin^2(\theta_m)$ in dependence of the order of maximum m (c.f. Fig. 12) yields a linear function, and from the slope the layer thickness d is obtained.

2. Experimental tasks, part 1

In part 1 of the experimental section, a SiGe pseudosubstrate will be analyzed by means of XRD. In particular, a reciprocal space map will be performed in order to determine the strain status and the Ge content of the SiGe pseudosubstrate. Here is the list of tasks:

1. Calculating the Bragg angle θ and the tilt angle ξ for the (004) and the (224) reflections of a Si(001) substrate
2. Mounting the SiGe pseudosubstrate onto the sample holder
3. Calibrating the z position of the sample
4. Calibrating ω , θ , and ξ to find the (0,0,4) reflection
5. Calibrating ω , θ , and ϕ to find the (2,2,4) reflection
6. Writing a job file that carries out the reciprocal space map around the (2,2,4) reflection
7. Performing the reciprocal space map

Prior to measuring the sample, it has to be mounted to the samples holder. Fig. 13 shows the mounted sample. The sample is attached to a quartz plate by adhesive tape. The quartz plate itself is attached to the tilt stage.

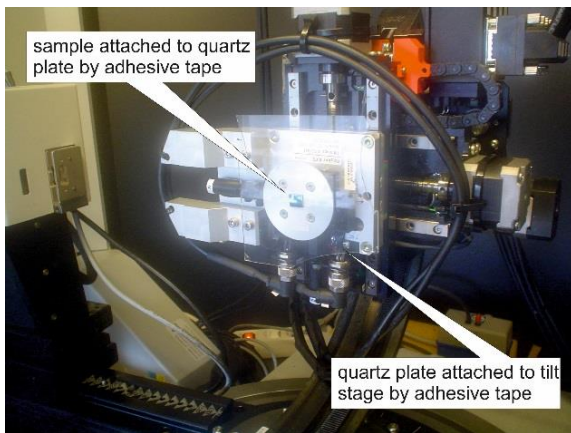


Fig 13: Sample and quartz plate mounted to the tilt stage of the XRD system.

Once the sample is mounted it has to be aligned with respect to the x-ray beam. Figure 14 shows a screen shot of the program Diffrac that is used to operate the XRD system. Before the alignment, make sure that the detector slit is set to 0.1 mm (label 1 in Fig. 13) to have a high detector resolution, and the angles theta and 2theta have to be at the zero position (label 2 and 3 in fig 14). Now the sample has to be moved into the x-ray beam by carrying a out a z drive scan (label 4 in figure 14). Punch the Start button to carry out the measurement. The sample is now moved towards you from outside the direct beam into the x-ray beam. As a result, the intensity is high at low z positions and it drops to zero once the sample hits the x-ray beam. Determine the position where the intensity is 50% and set the z position to this value.

In a second step, move the angle theta (angle of the sample, equivalent to ω) and 2theta (angle of the detector) to the nominal positions to find the (004) reflection. Now make a ω scan, i.e. a rocking curve (label 3 in Fig. 14) for a range of 2° with a resolution of 0.002° to find the (004) reflection. Set ω to the value, where the (004) peak is found. Now make a Chi scan to maximize the signal. In the third step, move theta and 2theta to find the (224) reflection. Again, make a rocking curve for a range of 2° with a resolution of 0.002° to find the peak. After that carry out a phi scan to maximize the signal.

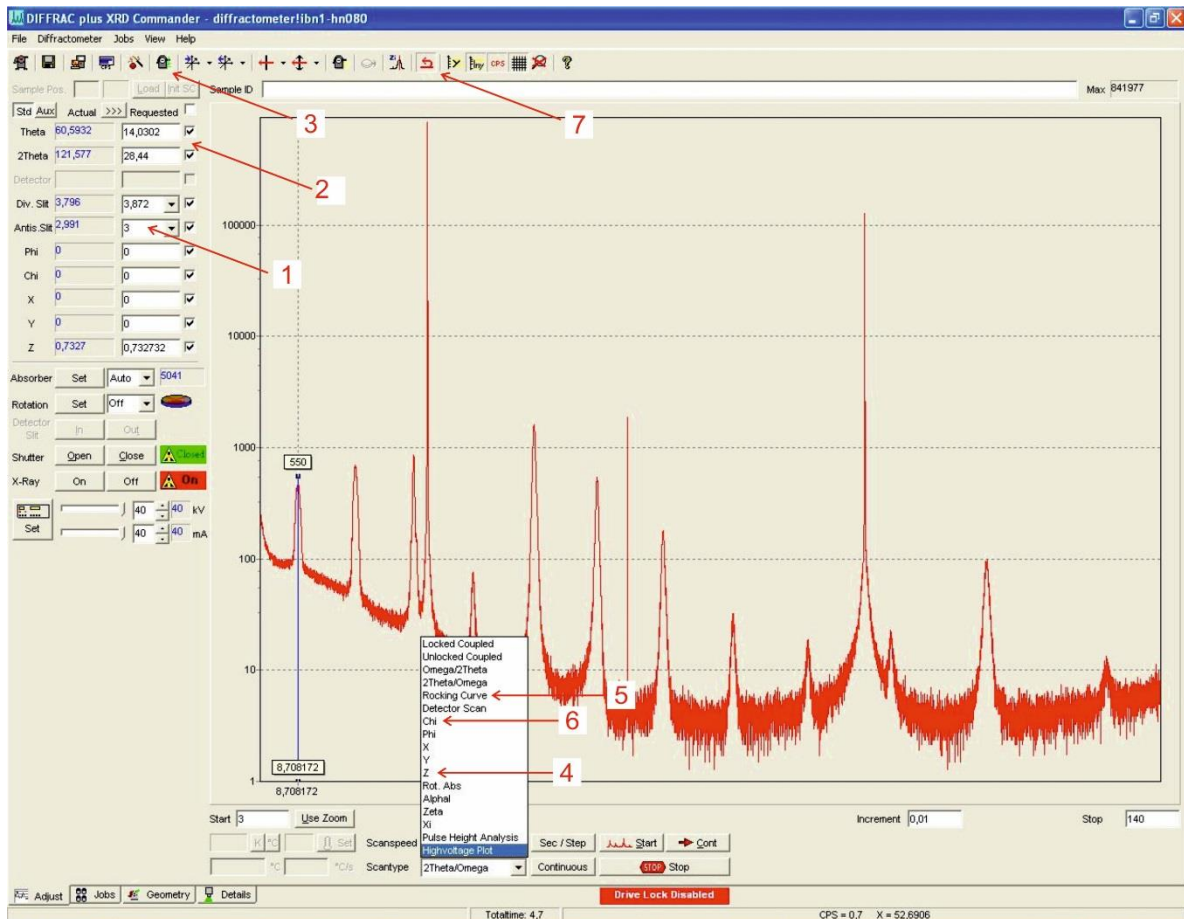


Fig 14: Screenshot of the Diffrac program that operates the Bruker D8 XRD system.

Once the angle ω , 2θ , χ and ϕ are set, a job file is created to carry out the reciprocal space map. The job file will be written by the supervisor. In the job file, the ranges in ω and $\omega/2\theta$ will be defined (c.f. figure 3):

Type of Scan	Relative start value	Relative end value	Resolution
ω scan	-0.5°	$+0.5^\circ$	0.02°
$\omega/2\theta$ scan	-2°	$+1^\circ$	0.02°

The scan will take 20 minutes. When finished the supervisor will convert the data to a text file that will be used by the students for the analysis.

3. Experimental tasks, part 2:

In part 2, a Si/SiGe superlattice will be analyzed by means of a $2\theta/\theta$ XRD scan. Here is a list of tasks:

1. Mounting the Si/SiGe superlattice onto the sample holder
2. Calibrating the z position of the sample
3. Calibrating ω , θ , and ξ to find the (0,0,4) reflection
4. Carrying out a $2\theta/\theta$ scan for a range $2\theta = 66^\circ - 71^\circ$ with a resolution of 0.002°

The mounting of the sample is similar to the experimental section 1. The scan will be carried out in continuous mode (button 7 in Fig. 14) for approximately 1 hour.

4. Experimental tasks, part 3

In part 3, a XRR measurement of a Bi_1Te_1 epilayer grown on a Si substrate is carried out:

1. Mounting the Bi_1Te_1 sample onto the holder
2. Calibrating the z position of the sample with detector slit of 0.1 mm
3. Carrying out a rocking curve in a range $-1^\circ - +1^\circ$ with a resolution of 0.01°
4. Setting the ω value to the maximum
5. Carrying out a $2\theta/\theta$ scan in a range $-0.2^\circ - +5^\circ$ with a resolution of 0.005°

5. Analyzing the data of part 1

The analysis of the data include:

1. Converting the raw data into reciprocal lattice vectors by means of the conversion_v2 code
2. Graphical visualization of the converted data in reciprocal space map
3. Determining the (k_x, k_z) values of the SiGe cap layer
4. Calculating the Ge content and the strain status $\varepsilon_{||}$ and ε_{\perp} of the SiGe cap layer

```
C:\User\Mussler\13-05-07\20130320b_annealedVN2_500_1s\RSM1\conversion_v2.m - Notepad++
Datei Bearbeiten Suchen Ansicht Format Sprachen Einstellungen Makro Ausfuehren TextFX Erweiterungen Fenster ?
conversion_v2.m
1 H = load('RSM1.dat');
2 N = length(H);
3 H2=zeros(N,3);
4
5 Theta=88.026028;
6 Omega=8.748624;
7 Reflection = [2 2 4];
8 range1=[-5 0.05 2];
9 range2=[-2 0.05 1];
10
11 H4 = zeros(N,3);
12 index=0;
13 for i = 1:N
14     if(H(i,3)==0 | H(i,3)<0 | H(i,3)>0)
15         index = index+1;
16         H4(index,:) = H(i,:);
17     end
18 end
19 H4=H4(1:index,:);
20
21 scannumber = H4(index,1);
22 if(scannumber~=H(N,1)),
23     range2(3)=(range2(3)-range2(1))/(H(N,1)-1)*(scannumber-1)+range2(1);
24 end
25
26 index4 = 1;
27 for i = 1:index
28     if(H4(i,1)~=index4)
29         scanweite = i-1;
```

Fig. 15: Screenshot of the program “conversion_v2.m” that is employed to calculate the reciprocal lattice vectors from the raw data file.

Concerning task 1, converting the raw data into reciprocal lattice vectors (equation 8 and 9), the students may use a self-written code "conversion_v2.m. This code runs under Matlab or Freemat (free program fully compatible to Matlab, it can be downloaded at <http://freemat.sourceforge.net>). A screenshot of the code is seen in Fig. 15. Mandatory to operate the code is to plug in several parameters of the reciprocal space map, i.e. the file name, the values of ω and 2θ , as well as the ranges of ω and $\omega/2\theta$. The code writes a text file "Ausgabe_q" that contains three columns of data ($k_{||}$, k_{\perp} , intensity).

Now the text file "Ausgabe_q" has to be visualized, i.e. a two-dimensional contour plot (k_x , k_y , I) has to be created. An example is depicted in figure 8b. The programs Origin or Matlab are quite useful here. Once the contour plot is done, determine the k_x and k_y coordinates of the SiGe cap layer peak. Determine the in-plane and out-of-plane lattice constants of the SiGe cap layer. By employing the equations described above, determine the Ge content and the strain status $\varepsilon_{||}$ and ε_{\perp} . For the latter two quantities, analytical calculations may be harnessed for a rough estimation or numerical methods may be employed for a precise determination.

6. Analyzing the data of part 2

Once the measurement of the XRD curve is finished, convert the raw file into a text file by means of the Leptos program. The text file contains a data row of two columns (2θ , I). Convert the 2θ values into reciprocal lattice vector (equation 9) and plot the intensity with respect to k_z . Determine the following parameters analytically:

1. Thickness $D = d_{\text{Si}} + d_{\text{SiGe}}$ of the SiGe/Si stack
2. Number of SiGe/Si periods

Besides the analytical calculations, the entire structure parameters will be analyzed by means of the simulation software "MadMax". Here is the list of tasks:

1. Reverting the experimental XRD data file from $(2\theta, I)$ to (θ, I)
2. Shifting the experimental data file, so that the substrate peak is at $\theta = 0^\circ$
3. Normalizing the Intensity to $I_{\text{max}} = 1$
4. Renaming the experimental data file to "filename.exp"
5. Inserting the SiGe/Si superlattice structure into MadMax (c.f. figure 11), starting with a guess
6. Saving the structure file as "filename.lay" in the same folder as the experimental file
7. Running the simulation by punching the "Sim + Exp" button
8. Changing the Si and SiGe thicknesses and the Si content to find a good agreement with the experimental data curve

Once, a good agreement between the experimental data and the simulation is found, plot the two curves in one graph ("MadMax" creates a file "filename.sim with the simulated XRD curve as an ASCII text).

7. Analyzing the data of part 3

The final goal of part 3 is to determine the thickness of the Bi_1Te_1 epilayer. The following tasks need to be done:

1. Converting the raw data into a text file ($2\theta, I$) in the Leptos program
2. Labelling the maxima according to the order m .
3. Determining the angular position θ_m of each maximum
4. Plotting $\sin^2(\theta_m)$ in dependence of m^2
5. Carrying out a linear regression to determine the slope.
6. Determine the thickness from the slope and the value δ (equation 21).